Desalination and Water Treatment
www.deswater.com

doi: 10.5004/dwt.2020.26179

202 (2020) 48–60
October

Applicability of the L^r form of the Kedem–Katchalsky–Peusner equations for membrane transport in water purification technology

Andrzej Ślęzak[a], Sławomir Grzegorczyn[b], Kornelia M. Batko[c], Wioletta M. Bajdur[a], Maria Włodarczyk-Makuła[d,*]

[a]*Department of Innovation and Safety Management Systems, Czestochowa University of Technology, 36b Armia Krajowa al, 42–200 Czestochowa, Poland, emails: aslezak52@gmail.com (A. Ślęzak), wiolawb@poczta.onet.pl (W.M. Bajdur)*
[b]*Department of Biophysics, Faculty of Medicine with the Division of Dentistry in Zabrze, Medical University of Silesia, 19 H. Jordan Str., 41808 Zabrze, Poland, email: grzegorczyn@sum.edu.pl (S. Grzegorczyn)*
[c]*Department of Informatics for Economics, University of Economics, 2B Bogucicka, 40287 Katowice, Poland, email: kornelia.batko@ue.katowice.pl (K.M. Batko)*
[d]*Department of Environmental Engineering, Czestochowa University of Technology, 69 Dabrowskiego Str., 42-200 Czestochowa, Poland, email: mwm@is.pcz.czest.pl (M. Włodarczyk-Makuła)*

Received 14 April 2020; Accepted 28 May 2020

ABSTRACT

Transport coefficients for the Nephrophan membrane in the horizontal plane and aqueous solutions of ethanol and glucose were calculated based on the Kedem–Katchalsky coefficients measured for homogeneous and non-homogeneous solutions. The calculated Peusner's coefficients for homogeneous solutions depend linearly while for non-homogeneous solutions nonlinearly on solute concentrations. In turn, coefficients ϕ_{ij}, describing the difference between configurations of the membrane system (*A* and *B*) point at the characteristic concentration 49.5 mol m^{-3}, for which the inflection point of dependencies of these coefficients as functions of solute concentration is observed. Besides newly defined coefficients, which normalize the Peusner's coefficients, depend nonlinearly on solute concentrations and for *A* configuration and non-homogeneous solutions increase of solute concentration causes increase while for *B* configuration decrease of these coefficients. The crisscross of suitable curves for *A* and *B* configuration is observed at 49.5 mol m^{-3}, for which the densities of solutions in the upper and lower chamber are the same. The presented mathematical description of membrane separation can be used for the analysis of the processes of water and wastewater treatment.

Keywords: Membrane transport; Non-electrolyte solutions; Peusner's network thermodynamics; Kedem–Katchalsky equations; Concentration polarization; Water technology

1. Introduction

The fundamental physical mechanisms of transmembrane transport substances have been studied in many areas of science (physics, biophysics, biology and chemistry) and technology [1–6]. One of the basic research tools of transport through membrane occurring in both the artificial and biological systems are Kedem–Katchalsky equations (K–K equations) [1,7] and non-dilute solute transport equation [8]. In practice for dilute solutions many versions of these equations are used: classical [9–12], mechanistic [13,14], and network forms of K–K equations [15]. These versions of the K–K equations show the relationships between volume

* Corresponding author.

1944-3994/1944-3986 © 2020 Desalination Publications. All rights reserved.

(J_v), solute (J_s) fluxes and thermodynamic forces (osmotic $\Delta\pi$ and/or hydrostatic ΔP). The degree of the coupling l results from the relationships between the forces and the fluxes for homogeneous solutions [1,15,16]. This degree for diluted and homogeneous binary solutions is defined by the relations $l_{12} = L_{12}(L_{11}L_{22})^{-0.5}$ and $l_{12} = l_{21} = l$. The second law of thermodynamic imposes $L_{11}L_{22}{}^{3} (L_{12})^2$, and therefore the l_{12} is limited by relation $-1 \le l \le +1$. When $l = \pm 1$, the system is completely coupled, the processes become a single process. When $l = 0$, the two processes are completely uncoupled and do not have any energy-conversion interactions. Taking into account the coefficient l, Kedem and Caplan [16] presented an expression for the maximum efficiency of energy conversion: $e_{max} = l^2[1 + (1 - l^2)^{0.5}]^{-2}$.

The network form of K–K equations was obtained by symmetrical and/or hybrid transformation of the classical K–K equations by use of Peusner network thermodynamics [15,17,18]. There are two symmetrical and two-hybrid forms of network K–K equations for homogeneous and non-homogeneous binary non-electrolyte solutions. The symmetrical forms of these equations include Peusner's coefficients: R_{ij} and L_{ij} (for homogeneous solutions) and R^*_{ij} and L^*_{ij} (for non-homogeneous solutions) while the hybrid forms include Peusner's coefficients: P_{ij} and H_{ij} (for homogeneous solutions) and P^*_{ij} and H^*_{ij} (for non-homogeneous solutions) ($i, j \in \{1, 2\}$) [17,19–21]. There are two symmetrical and six hybrid forms of network K–K equations for homogeneous ternary non-electrolyte solutions. Symmetrical forms of these equations, as in the case of binary solutions include Peusner's coefficients R_{ij} or L_{ij} while hybrid forms – Peusner's coefficients H_{ij}, N_{ij}, K_{ij}, P_{ij}, S_{ij} or W_{ij} ($i, j \in \{1, 2, 3\}$) [18]. It should be noted that the coefficients R_{ij} and L_{ij} are directly derived from Onsager's reciprocal rules while the remaining coefficients are the consequence of the use of techniques of network thermodynamics [15,17].

In the previous paper [22] the case of two-directional tri-port of Peusner's network thermodynamics with single inputs for volume flux J^r_v coupled with thermodynamic force $\Delta P - \Delta\pi_1 - \Delta\pi_2$ and solute fluxes: J^r_1 coupled with thermodynamic force $\Delta\pi_1/\bar{C}_1$ and J^r_2 coupled with thermodynamic force $\Delta\pi_2/\bar{C}_2$ was considered. The network K–K equations for non-homogeneous ternary non-electrolyte solutions containing Peusner's coefficients H^r_{ij} ($i, j \in \{1, 2, 3\}$, $r = A, B$) were obtained by means of hybrid network transformations of Peusner's network thermodynamic. The coefficients H^r_{ij} ($i, j \in \{1, 2, 3\}$, $r = A, B$) occurring in the matrix $[H^r]$ we call Peusner's coefficients and matrix $[H^r]$ – matrix of Peusner's coefficients H^r_{ij}. According to the principles of network thermodynamic, for non-diagonal coefficients, we have $H^r_{12} \ne H^r_{21}$, $H^r_{13} \ne H^r_{31}$ and $H^r_{23} \ne H^r_{32}$.

The aim of this work is to develop the form of L^r of the K–K equations, containing the Peusner coefficients L^r_{ij} ($i, j \in \{1, 2, 3\}$, $r = A, B$). The results of calculations of coefficients L^r_{ij} and L_{ij} matrix coefficients $L^r_{det} = \det[L^r]$ and $L_{det} = \det[L]$ and the quotients $\phi_{ij} = (L^A_{ij} - L^B_{ij})/L_{ij}$ and $\phi_{det} = (L^A_{det} - L^B_{det})/L_{det}$ will be presented, obtained on the basis of experimentally determined coefficients (L_p, s_1, s_2, ω_{11}, ω_{22}, ω_{21}, ω_{12}, ζ^r_1 and ζ^r_2 for glucose in aqueous ethanol solutions and configurations A and B (Fig. 1) of the membrane system. These coefficients were calculated on the basis of experimentally measured volume (J^r_v) and solute fluxes (J^r_k) ($k = 1, 2$ and $r = A, B$) using the procedure described in [7,23]. Besides the results of calculations of the degree of coupling $l_{ij} = L_{ij}(L_{ii}L_{jj})^{-0.5}$ (for homogeneous ternary non-electrolyte solutions), $l^r_{ij} = L^r_{ij}(L^r_{ii}L^r_{jj})^{-0.5}$ (for non-homogeneous ternary non-electrolyte solutions) and energy conversion coefficients $(e_{ij})_l = (l_{ji})^2[1 + (1 - l_{ij}l_{ji})^{0.5}]^{-2}$ (for homogeneous ternary non-electrolyte solutions) and $(e^r_{ij})_l = (l^r_{ji})^2\,[1 + (1 - l^r_{ij}l^r_{ji})^{0.5}]^{-2}$ (for non-homogeneous ternary non-electrolyte solutions), in which ($i, j \in \{1, 2, 3\}$, $r = A, B$) will be presented.

2. Materials and methods

2.1. Membrane system

Similarly, as in previous paper [22], transport through the single-membrane system will be considered, wherein the membrane (M) separates compartments (l) and (h) filled with non-homogeneous ternary non-electrolyte solutions with concentrations at the initial moment ($t = 0$) C_{kh} and C_{kl} ($C_{kh} > C_{kl}$, $k = 1, 2$) (Fig. 1).

This membrane is a "black box" type for solvent and non-electrolyte dissolved substances [24]. In the case of membrane located in a horizontal plane that is perpendicular to the gravity vector, there are A and B configurations of solutions arrangement in relation to the membrane

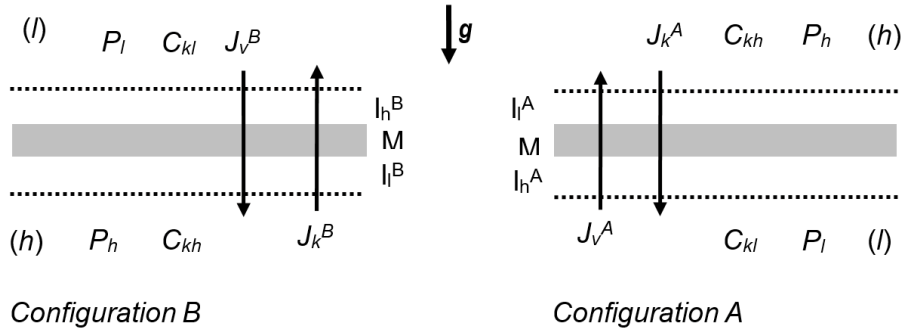

Fig. 1. Model of the single-membrane system: M – membrane, l^A_l and l^A_h – the concentration boundary layers in configuration A, l^B_l and l^B_h – the concentration boundary layers in configuration B, P_h and P_l – mechanical pressures, C_{kh} and C_{kl} – concentrations of solutions, J^A_k and J^A_v – solute and volume fluxes in configuration A, J^B_k and J^B_v – solute and volume fluxes in configuration B, $\bar{g}$ – the gravitational acceleration.

(r = A or B). In A configuration the solution with greater ethanol concentration C_{2h} is in the chamber over the membrane while the solution with lower ethanol concentration C_{2l} – in a chamber under the membrane. In B configuration of the membrane system location of solutions is reversed. The sign of the flux is depended on its direction in relation to gravitational acceleration. The flux is positive when is directed as gravitational acceleration and negative when is directed in opposite direction to the gravity vector.

2.2. Measuring system

Experimental studies of volume (J_v^r) and solutes (J_k^r, k = 1, 2) fluxes through a horizontally oriented membrane were carried out by means of the measurement set-up described in detail in previous papers [24]. The membrane (M) with a surface area equal to 3.36 cm^2 was placed between two Plexiglass vessels (l, h), each with a volume of 0.2 l. For this purpose, we used the measuring system that consisted of the Nephrophan membrane located in a horizontal plane separated two aqueous glucose (subscript 1) and ethanol (subscript 2) solutions with concentrations C_{h1} = 101÷1 mol m^{-3}, C_{l1} = 1÷101 mol m^{-3}, C_{h2} = 201 mol m^{-3} and C_{l2} = 1 mol m^{-3}. The Nephrophan membrane is the microporous, highly hydrophilic polymeric filter used in medicine (VEB Filmfabrik, Wolfen, Germany). This membrane is made of cellulose acetate (cello-triacetate $(OCO–CH_3)_n$). The electron microscope image of the surface and cross-section of this membrane was presented in Ślęzak et al. [24]. Therefore, we obtained the differences in osmotic pressures in the range from Δp_1 = −245.1 kPa to Δp_1 = +245.1 kPa and Δp_2 = ±490.3 kPa. The vessel (h) was coupled with a calibrated pipette, while the vessel (l) was connected to an external reservoir of solution. The volume (J_v^r) and solute (J_k^r, k = 1, 2) fluxes were determined respectively as $J_v^r = S^{-1}dV^r/dt$ and $J_k^r = V_l S^{-1}dC^r/dt$, where S is the membrane surface area and dV^r/dt is the volume change (V) occurring in time (t), V_l is the volume of the measuring vessel and dC^r/dt is the concentration change (dC) occurring in time (dt). Superscript r = A, B refer to configuration A and B of the membrane system. Measurements of J_v^r and J_k^r for configuration A (r = A) or B (r = B) were taken according to the following procedure [23]. The first step involved the measurement of J_v^r and J_k^r in the membrane system with mechanical stirring of solutions at 500 rpm. After achieving the steady-state during which $J_v(t)$ and $J_k(t)$ were constant, stirring was stopped and subsequently the evolution of $J_v^r(t)$ and $J_k^r(t)$ were measured up to a steady-state, in which J_v^r and J_k^r (r = A, B) were constant. The fluxes J_v and J_v^r are always directed from the solution with a lower concentration to a solution of higher concentration and the fluxes J_k and J_k^r in the opposite direction, regardless of the configuration of the membrane system. The measurement error of the fluxes did not exceed 5% and the solution preparation error – 1%.

2.3. L^r form of the Kedem–Katchalsky equations for non-homogenous non-electrolyte ternary solutions

According to the Kedem–Katchalsky formalism [7,23] transport properties of the membrane for solutions containing a solvent and dissolved two substances are determined by coefficients: hydraulic permeability (L_p), reflection (σ_k, k = 1, 2) and permeability of solute (ω_{kf}, $k, f \in \{1, 2\}$). In turn, the transport properties of the complex $l_l^r/M/l_h^r$ are characterized by coefficients of hydraulic permeability (L_{ij}^r), reflection (σ_{sk}^r, σ_{ak}^r) and permeability of solute (ω_{kf}^r). The coefficients of hydraulic, osmotic, advective and diffusive concentration polarization are defined by expressions: $\zeta_p^r = L_p^r/L_p$, $\zeta_v^r = \sigma_{sk}^r/\sigma_{sk}$, $\zeta_a^r = \sigma_{ak}^r/\sigma_{ak}$ and $\zeta_s^r = \omega_{kf}^r/\omega_{kf}^r$ [17]. For osmotic volume and diffusive fluxes of homogeneous (evenly stirred) solutions, the values of volume (J_v) and solutes (J_k) fluxes do not depend on the configuration of the membrane system. Besides the dependencies $J_v = f(C_{kh} - C_{kl})$ and $J_k = f(C_{kh} - C_{kl})$ are linear, while $J_v^r = f(C_{kh} - C_{kl})$ and $J_k^r = f(C_{kh} - C_{kl})$ – nonlinear [25]. The appearance of the layers δ_h^r and δ_l^r reduce the value of volume and solute fluxes from J_v and J_k (in conditions of homogeneous solutions) to J_v^r and J_k^r (in the condition of concentration polarization), respectively [23].

The classical K–K equations for concentration polarization conditions can be written as Eqs. (1)–(3):

$$J_v^r = \zeta_p^r L_p \left(\Delta P - \zeta_{v1}^r \sigma_1 \Delta\pi_1 - \zeta_{v2}^r \sigma_2 \Delta\pi_2\right) \tag{1}$$

$$J_1^r = \zeta_{s11}^r \omega_{11} \Delta\pi_1 + \zeta_{s12}^r \omega_{12} \Delta\pi_2 + \bar{C}_1 \left(1 - \zeta_{\alpha 1}^r \sigma_1\right) J_v^r \tag{2}$$

$$J_2^r = \zeta_{s21}^r \omega_{21} \Delta\pi_1 + \zeta_{s22}^r \omega_{22} \Delta\pi_2 + \bar{C}_2 \left(1 - \zeta_{\alpha 2}^r \sigma_2\right) J_v^r \tag{3}$$

where J_v^r, J_1^r and J_2^r – volume and solutes "1" and "2" fluxes respectively, L_p – hydraulic permeability coefficient, σ_1 and σ_2 – reflection coefficients suitably for solutes "1" and "2", ω_{11} and ω_{22} – solute permeability coefficients for solutes "1" and "2" connected with forces with indexes "1" and "2" and ω_{12} and ω_{21} – cross coefficients of permeability for substances "1" and "2" connected with forces with indexes "2" and "1" respectively. $\Delta P = P_h - P_l$ is the hydrostatic pressure difference (P_h, P_l are higher and lower values of hydrostatic pressure suitably). $\Delta\pi_k = RT(C_{kh} - C_{kl})$ is the difference of osmotic pressure (RT is the product of gas constant and thermodynamic temperature).

For the conditions of concentration polarization illustrated in Fig. 1, by the introduction of a matrix [L^r] and fluxes J_v^r, J_1^r and J_2^r, the Eqs. (1)–(3) take the following form:

$$\begin{bmatrix} J_v^r \\ J_1^r \\ J_2^r \end{bmatrix} = \begin{bmatrix} L_{11}^r & L_{12}^r & L_{13}^r \\ L_{21}^r & L_{22}^r & L_{23}^r \\ L_{31}^r & L_{32}^r & L_{33}^r \end{bmatrix} \begin{bmatrix} \Delta P - \Delta\pi_1 - \Delta\pi_2 \\ \dfrac{\Delta\pi_1}{\bar{C}_1} \\ \dfrac{\Delta\pi_2}{\bar{C}_2} \end{bmatrix} = \left[L^r\right] \begin{bmatrix} \Delta P - \Delta\pi_1 - \Delta\pi_2 \\ \dfrac{\Delta\pi_1}{\bar{C}_1} \\ \dfrac{\Delta\pi_2}{\bar{C}_2} \end{bmatrix} \tag{4}$$

where $L_{11}^r = \zeta_p^r L_p$, $L_{12}^r = \zeta_p^r L_p (1 - \sigma_1 \zeta_v^r) \bar{C}_1$, $L_{13}^r = \zeta_p^r L_p (1 - \sigma_2 \zeta_v^r) \bar{C}_2$, $L_{21}^r = \zeta_p^r L_p (1 - \sigma_1 \zeta_{a1}^r) \bar{C}_1$, $L_{22}^r = \zeta_{s11}^r \omega_{11} \bar{C}_1 + \zeta_p^r L_p (1 - \sigma_1 \zeta_{a1}^r)(1 - \sigma_1 \zeta_v^r) \bar{C}_1^2$, $L_{23}^r = \zeta_{s12}^r \omega_{12} \bar{C}_2 + \zeta_p^r L_p (1 - \sigma_1 \zeta_{a1}^r)(1 - \sigma_2 \zeta_v^r) \bar{C}_1 \bar{C}_2$, $L_{31}^r = \zeta_p^r L_p (1 - \sigma_2 \zeta_{a2}^r) \bar{C}_2$, $L_{32}^r = \zeta_{s21}^r \omega_{21} \bar{C}_1 + \zeta_p^r L_p (1 - \sigma_2 \zeta_{a2}^r)(1 - \sigma_1 \zeta_v^r) \bar{C}_1 \bar{C}_2$, $L_{33}^r = \zeta_{s22}^r \omega_{22} \bar{C}_2 + \zeta_p^r L_p (1 - \sigma_2 \zeta_{a2}^r)(1 - \sigma_2 \zeta_v^r) \bar{C}_2^2$, [$L^r$] is the matrix of Peusner's coefficients for ternary non-electrolyte solutions in conditions

of concentration polarization. Determinant of matrix $[L^r]$ can be written in the form:

$$\det\left[L^r\right] = L^r_{\det} = \zeta^r_p L_p C_1 C_2 \left(\zeta^r_{s11}\zeta^r_{s22}\omega_{11}\omega_{22} - \zeta^r_{s12}\zeta^r_{s21}\omega_{12}\omega_{21}\right) \quad (5)$$

Taking into consideration Eq. (4) we get: $L^r_{12} \neq L^r_{21}$, $L^r_{13} \neq L^r_{31}$ and $L^r_{23} \neq L^r_{32}$. This shows that for conditions of concentration polarization Onsager's reciprocal relations is not satisfied, according to which it should be $L^r_{ij} = L^r_{ji}$[15]. In order to determine the conditions in which this hypothesis is fulfilled we calculate the following ratios $L^r_{12}/L^r_{21} = (1 - \sigma_1\zeta^r_v)/(1 - \sigma_1\zeta^r_{a1})$, $L^r_{13}/L^r_{31} = (1 - \sigma_2\zeta^r_v)/(1 - \sigma_2\zeta^r_{a2})$ and $L^r_{23}/L^r_{32} = [\zeta^r_{s12}\omega_{12}\bar{C}_2 + \zeta^r_p L_p(1 - \sigma_1\zeta^r_{a1})(1 - \sigma_2\zeta^r_v)\bar{C}_1\bar{C}_2]/[\zeta^r_{s21}\omega_{21}\bar{C}_1 + \zeta^r_p L_p(1 - \sigma_2\zeta^r_{a2})(1 - \sigma_1\zeta^r_v)\bar{C}_1\bar{C}_2]$. From these equations, it follows that $L^r_{12} = L^r_{21}$ and $L^r_{13} = L^r_{31}$, if $\zeta^r_{v1} = \zeta^r_{a1} = \zeta^r_1$, $\zeta^r_{v2} = \zeta^r_{a2} = \zeta^r_2$ or $\sigma_1 = \sigma_2 = 0$. Similarly if $\zeta^r_v = \zeta^r_{a1} = \zeta^r_{a2} = \zeta^r_p = \zeta^r_{s12} = \zeta^r_{s21} = \zeta^r_{s11} = \zeta^r_{s22} = \zeta^r$ or $\sigma_1 = \sigma_2 = 0$ and $\omega_{12}\bar{C}_2 = \omega_{21}\bar{C}_1$, then $L^r_{23} = L^r_{32}$.

The coefficients L^r_{ij} ($i, j \in \{1, 2, 3\}$, $r = A, B$) and $\det[L^r]$ were calculated for polymer membrane Nephrophan and glucose in an aqueous solution of ethanol using Eqs. (4) and (5). In expressions under Eq. (4) which describe the matrix coefficients L^r_{11}, L^r_{12}, L^r_{13}, L^r_{21}, L^r_{22}, L^r_{23}, L^r_{31}, L^r_{32} and L^r_{33}, there are coefficients that describe transport properties of the membrane (L_p, s_1, s_2, ω_{11}, ω_{22}, ω_{21} and ω_{12}), average concentrations of solutions "1" and "2" in the membrane ($\bar{C}_1$, $\bar{C}_2$) and coefficients of concentration polarization (ζ^r_v, ζ^r_{a1}, ζ^r_{a2}, ζ^r_p, ζ^r_{s12}, ζ^r_{s21}, ζ^r_{s11} and ζ^r_{s22}).

The network K–K equations for homogeneous ternary non-electrolyte solutions containing Peusner's coefficients L_{ij} ($i, j \in \{1, 2\}$) were obtained by means of symmetrical network transformations of Peusner's thermodynamic. This equation can be written in the form:

$$\begin{bmatrix} J_v \\ J_1 \\ J_2 \end{bmatrix} = \begin{bmatrix} L_{11} & L_{12} & L_{13} \\ L_{21} & L_{22} & L_{23} \\ L_{31} & L_{32} & L_{33} \end{bmatrix} \begin{bmatrix} \Delta P - \Delta\pi_1 - \Delta\pi_2 \\ \dfrac{\Delta\pi_1}{\bar{C}_1} \\ \dfrac{\Delta\pi_2}{\bar{C}_2} \end{bmatrix} = \left[L^r\right] \begin{bmatrix} \Delta P - \Delta\pi_1 - \Delta\pi_2 \\ \dfrac{\Delta\pi_1}{\bar{C}_1} \\ \dfrac{\Delta\pi_2}{\bar{C}_2} \end{bmatrix} \quad (6)$$

where $L_{11} = L_p$, $L_{12} = L_p(1 - \sigma_1)\bar{C}_1 = L_{21}$, $L_{13} = L_p(1 - \sigma_2)\bar{C}_2 = L_{31}$, $L_{22} = \omega_{11}\bar{C}_1 + L_p(1 - \sigma_1)^2\bar{C}_1^2$, $L_{23} = \omega_{12}\bar{C}_2 + L_p(1 - \sigma_1)(1 - \sigma_2)\bar{C}_1\bar{C}_2$, $L_{32} = \omega_{21}\bar{C}_1 + L_p(1 - \sigma_1)(1 - \sigma_2)\bar{C}_1\bar{C}_2^1 L_{23}$, $L_{33} = \omega_{22}\bar{C}_2 + L_p(1 - \sigma_2)^2\bar{C}_2^2$, J_v – volume flux, J_{s1} and J_{s2} – fluxes of solute "1" and "2" through the membrane in conditions of homogeneous solutions, L_p – coefficient of hydraulic permeability, σ_1 and σ_2 – reflection coefficients suitably for solutes "1" and "2", ω_{11} and ω_{22} – solute permeability coefficients for solutes "1" and "2" connected with forces with indexes "1" and "2" and ω_{12} and ω_{21} – cross coefficients of permeability for substances "1" and "2" connected with forces with indexes "2" and "1" suitably. Besides the determinant of the matrix $[L]$ is given by the relationship:

$$\det\left[L\right] = L_{\det} = L_p C_1 C_2 \left(\omega_{11}\omega_{22} - \omega_{12}\omega_{21}\right) \quad (7)$$

Eqs. (6) and (7) can be applied to a system in which the membrane separates two homogeneous solutions (evenly stirred). This situation is idealized, especially in biological systems. In real conditions, we should take into consideration the phenomenon of concentration polarization of membrane relying on the creation of concentration boundary layers (CBLs) on both sides of the membrane [27,29]. The above equation does not include this case. Index "r" indicates that coefficients L^r_{ij} and matrix $[L^r]$ of these coefficients depend on the configuration of the membrane system.

In order to show the relations between coefficients L^r_{ij} and L_{ij} and between determinants of matrixes $[L^r]$ and $[L]$ for A and B configurations of the membrane system ($r = A, B$), using Eqs. (4), (7)–(9) will be calculated.

$$\phi_{ij} = \frac{L^A_{ij} - L^B_{ij}}{L_{ij}} \quad (8)$$

$$\phi_{\det} = \frac{\det\left[L^A\right] - \det\left[L^B\right]}{\det\left[L\right]} \quad (9)$$

The values of coefficients ϕ_{ij} and $\phi_{\det}$ shows the influence of concentration polarization and natural convection on the membrane transport. These coefficients are a measure of the distance of convective processes from the critical state (non-convection) and fulfill the criterion: $-1 \leq \phi_{ij}, \phi_{\det} \leq 1$. In the critical state $\phi_{ij} = \phi_{\det} = 0$. This means that $L^A_{ij} = L^B_{ij}$ ($i, j \in \{1, 2, 3\}$ and $L^A_{\det} = L^B_{\det}$. The condition $\phi_{ij} = \phi_{\det} = +1$ is fulfilled if $L^A_{ij} = L^A_{\det} = 0$ and $L^B_{ij} = L^B_{\det} = L_{ij} = L_{\det}$. In turn, $\phi_{ij} = \phi_{\det} = +1$, is satisfied if $L^B_{ij} = L^B_{\det} = 0$ and $L^A_{ij} = L^A_{\det} = L_{ij} = L_{\det}$.

In order to show the relation between coefficients L_{ij}, L_{ji}, L_{ii} and L_{jj} and coefficients L^r_{ij}, L^r_{ji}, L^r_{ii} and L^r_{jj} for A and B configurations of membrane system we will calculate the Kedem–Caplan–Peusner degree of coupling l_{ij} and l^r_{ij}, in which $i, j \in \{1, 2, 3\}$, $r = A, B$, using Eqs. (1) and (4) [15,16]. The expressions for these coefficients take the following forms:

$$l_{ij} = \frac{L_{ij}}{\sqrt{L_{ii}L_{jj}}} \quad (10)$$

$$l^r_{ij} = \frac{L^r_{ij}}{\sqrt{L^r_{ii}L^r_{jj}}} \quad (11)$$

Taking into consideration Eqs. (4), (6), (10) and (11) we get: $l^r_{12} \neq l^r_{21}$, $l^r_{13} \neq l^r_{31}$, $l_{23} \neq l_{32}$ and $l^r_{23} \neq l^r_{32}$. This shows that for conditions of concentration polarization Onsager's reciprocal relations are not satisfied.

The l^r_{ij} coefficients can be used to evaluate energy conversion efficiency by means of Kedem–Caplan–Peusner coefficient, which can be written in the form:

$$e_{ij} = \frac{\left(l_{ji}\right)^2}{\left(1 + \sqrt{1 - l_{ij}l_{ji}}\right)^2} = \frac{\left(L_{ji}\right)^2}{L_{ii}L_{jj}\left(1 + L_{ii}L_{jj}\sqrt{L_{ii}L_{jj} - L_{ij}L_{ji}}\right)^2} \quad (12)$$

$$e^r_{ij} = \frac{\left(l^r_{ji}\right)^2}{\left(1 + \sqrt{1 - l^r_{ij}l^r_{ji}}\right)^2} = \frac{\left(L^r_{ji}\right)^2}{L^r_{ii}L^r_{jj}\left(1 + L^r_{ii}L^r_{jj}\sqrt{L^r_{ii}L^r_{jj} - L_{ij}L_{ji}}\right)^2} \quad (13)$$

3. Results and discussion

3.1. Experiments

3.1.1. Concentration dependencies J_v^r and J_k^r for ternary solutions

The dependencies of volume fluxes in non-homogeneous (J_v^r) and homogeneous (J_v) conditions as functions of glucose osmotic pressure ($\Delta\pi_1$) with constant values of $\Delta P = 0$, $\Delta\pi_2 = 490.3$ kPa and for *A* (graphs 2 and 4) and *B* (graphs 1 and 3) configurations of the membrane system are presented in Fig. 2.

Graphs 1 and 2 presented in this figure were obtained when the solutions were not mechanically stirred (non-homogeneous conditions – the case of concentration polarization of the membrane), whereas graphs 3 and 4 in this figure were obtained for the case of mechanically stirred solutions at 500 rpm (homogeneous conditions). The dependencies $J_v = f(\Delta\pi_1)$ (graphs 3 and 4) are linear, whereas the dependencies $J_v^r = f(\Delta\pi_1)$ (graphs 1 and 2) are nonlinear. Besides the main nonlinear change of graphs 1 and 2 are observed in different ranges of glucose concentration for different configurations of the membrane system. In these cases, the appearance of CBLs near the membrane disturbs membrane transport. For the change of configurations of the membrane systems the case in which the difference of density causes change of diffusive conditions into diffusive and convective conditions depends on the case in which the density over the membrane is greater than under the membrane. Because the change of configuration from *A* to *B* also reverses the solutions in relation to the membrane we observe the range of nonlinear changes of volume flux for positive glucose osmotic pressure in one configuration and negative for the second.

Analogically, the dependencies of solute fluxes J_k^r and J_k (k = 1, 2 and r = *A*, *B*) as functions of glucose osmotic pressure for constant $\Delta P = 0$, $\Delta\pi_2 = 490.3$ kPa and for *A* (graphs 2 and 4) and *B* (graphs 1 and 3) configurations of the membrane system are presented in Figs. 3 and 4.

Similarly as for volume flux concentration characteristics of solute fluxes: for glucose (Fig. 3) and ethanol (Fig. 4) for non-stirred solutions are different for different configurations. The nonlinear ranges of these characteristics are similar to volume fluxes, this indicates the main reason for these nonlinearities – the change of conditions of CBLs rebuilding from diffusional to diffusional and convective.

In the previous papers [26,27,29] we show that in terms of concentration polarization (non-convective state) volume J_v^r and solute J_k^r fluxes reach minimum values. In configuration

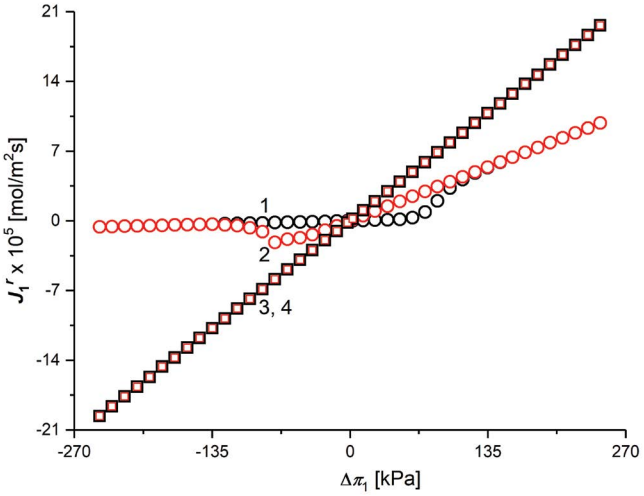

Fig. 3. Glucose fluxes as functions of osmotic pressure difference of glucose with a constant osmotic pressure of ethanol for $\Delta\pi_2 = 490.3$ kPa and $\Delta P = 0$: for not stirred solutions (1) and (2), for stirred solutions (3) and (4). Configurations of the membrane system: *A* – graphs (2) and (4), *B* – graphs (1) and (3).

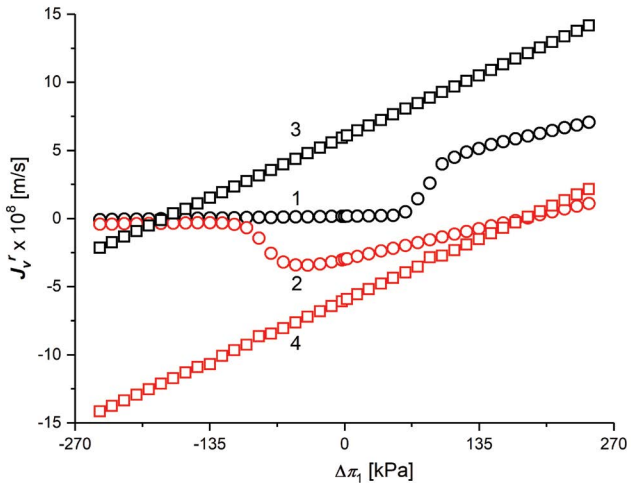

Fig. 2. Volume fluxes as functions of the osmotic pressure of glucose with a constant osmotic pressure of ethanol $\Delta\pi_2 = 490.3$ kPa and $\Delta P = 0$: for not stirred solutions (1) and (2) and stirred solutions (3) and (4). Configurations of membrane system: *A* – graphs (2) and (4), *B* – graphs (1) and (3).

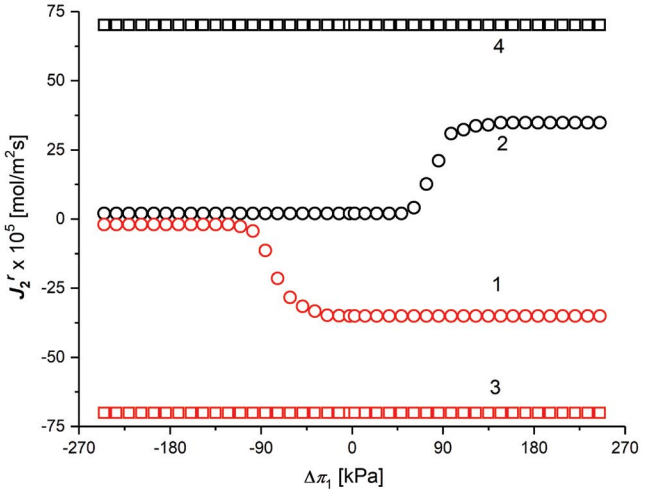

Fig. 4. Ethanol fluxes as functions of osmotic pressure difference of glucose with a constant osmotic pressure of ethanol $\Delta\pi_2 = 490.3$ kPa and $\Delta P = 0$: for not stirred solutions (1) and (2), for stirred solutions (3) and (4). Configurations of the membrane system: *A* – graphs (2) and (4), *B* – graphs (1) and (3).

A, a non-convective state occurs when the density of the solution in the compartment above the membrane is higher than the density of the solution in the compartment under the membrane. Natural convection increases the values of fluxes J_v^r and J_k^r.

3.1.2. Concentration dependencies of concentration polarization coefficients

In the previous papers [25,29] it has been shown that for polymer membrane Nephrophan and aqueous solutions of glucose the dependencies $\zeta_p^r = \zeta_{a1}^r = \zeta_{a2}^r = 1$, $\zeta_{s11}^r = \zeta_{s12}^r = \zeta_1^r$ and $\zeta_{s22}^r = \zeta_{s21}^r = \zeta_2^r$ are fulfilled. Thus, the membrane transport parameters determined experimentally are equal to: $L_p = 4.9 \times 10^{-12}$ m^3 N^{-1} s^{-1}, $s_1 = 0.07$, $s_2 = 0.025$, $\omega_{11} = 0.8 \times 10^{-9}$ mol N^{-1} s^{-1}, $\omega_{12} = 0.81 \times 10^{-13}$ mol N^{-1} s^{-1}, $\omega_{22} = 1.43 \times 10^{-9}$ mol N^{-1} s^{-1} and $\omega_{21} = 1.63 \times 10^{-12}$ mol N^{-1} s^{-1} [25]. The polarization coefficients ζ_v^r, ζ_1^r and ζ_2^r (for constant values of $\bar{C}_2 = 37.7$ mol m^{-3}) as functions of mean glucose concentration in membrane ($\bar{C}_1$), for configurations *A* and *B* of the membrane system are shown in Fig. 5.

In the case of configuration *A* for $\bar{C}_1 \leq 45.5$ mol m^{-3}, $\zeta_1^A = \zeta_2^A = \zeta_v^A = 0.03 = \text{const.}$, and for $\bar{C}_1 > 45.5$ mol m^{-3} the values of coefficients ζ_1^A, ζ_2^A and ζ_v^A increase nonlinearly with glucose concentration increase and for $\bar{C}_1 > 50.96$ mol m^{-3} reach constant value equal respectively to $\zeta_1^A = \zeta_2^A = \zeta_v^A = 0.5 = \text{const.}$ In the case of configuration *B* for $\bar{C}_1 \leq 45.5$ mol m^{-3}, $\zeta_1^B = \zeta_2^B = \zeta_v^B = 0.5 = \text{const.}$, and for $\bar{C}_1 > 45.5$ mol m^{-3} the values of coefficients ζ_1^B, ζ_2^B and ζ_v^B decrease with increase of glucose concentration and for $\bar{C}_1 > 50.96$ mol m^{-3} reach constant value equal respectively to $\zeta_1^B = \zeta_2^B = \zeta_v^B = 0.03$.

In addition, for $\bar{C}_1 < 45.5$ mol m^{-3} in configuration *A* the CBLs complex is stable and in the *B* configuration – hydrodynamically unstable. The reason is the predominance of ethanol concentration over glucose in solutions separated by the membrane. This causes the convective movements of the solutions. In configuration *B*, for $\bar{C}_1 < 45.5$ mol m^{-3}, the layers near membrane surfaces are unstable, because the density of the solution under the membrane is greater than the solution above the membrane. In the configuration *A*, for $\bar{C}_1 > 45.5$ mol m^{-3}, the CBLs complex is destabilized and in the *B* configuration, for $\bar{C}_1 > 45.5$ mol m^{-3} – the complex of CBLs reaches hydrodynamic stabilization. The reason is the predominance of glucose over ethanol in solutions separated by the membrane. Therefore, the density of the solution under the membrane is greater than over the membrane. For $\bar{C}_1 = 49.2$ mol m^{-3} complex of CBLs is independent of the configuration of the membrane system and therefore $\zeta_1^A = \zeta_2^A = \zeta_v^A = \zeta_1^B = \zeta_2^B = \zeta_v^B = 0.23$.

From Fig. 5 it results that concentration polarization coefficients are sensitive to the configuration of the membrane system. For this same configuration, the dependencies of concentration polarization coefficients as functions of glucose concentration are similar (only slightly different from each other). The main feature of these dependencies is that for one of configuration (*A*) the values of coefficients start from low values for small glucose concentration and after the range with small changes of coefficients, but above 48 mol m^{-3} the glucose concentration increase causes that coefficients values increase with greater inclination. For other configuration of the membrane system (*B*) the coefficients of concentration polarization are high for small glucose concentration and do not change up to 48 mol m^{-3} glucose concentration, for glucose concentrations higher than 48 mol m^{-3} increase of glucose concentration causes a decrease of concentration polarization coefficients. The crisscross of the above-discussed characteristics for *A* and *B* configuration (observed at 49.3 mol m^{-3} glucose concentration) can be the point of identification of change of conditions of CBLs rebuilding.

3.2. Calculations of the coefficients L_{ij}^r, L_{det}^r ($i, j \in \{1, 2, 3\}$, $r = A, B$)

The coefficients L_{ij}^r ($i, j \in \{1, 2, 3\}$, $r = A, B$), determinant of matrix of these coefficients $\det[L^r] = L_{\det}^r$ were calculated based on Eqs. (4)–(7), transport parameters for Nephrophan membrane and presented in Figs. 6–9. The values of coefficients $L_{11}^A = L_{11}^B = L_{11} = 4.9 \times 10^{-12}$ m^3 N^{-1} s^{-1}, calculated on the bases of Eqs. (4) and (6) are constant and do not depend on both $\bar{C}_1$ and $\bar{C}_2$ and the configuration of the membrane system. Similarly $L_{31}^A = L_{31}^B = L_{31} = 1.8 \times 10^{-10}$ mol N^{-1} s^{-1}.

The graphs 1A, 1B, 1, 2A, 2B and 2 presented in Fig. 6 illustrate the dependencies $L_{12}^r = f(\bar{C}_1, \bar{C}_2 = 37.71 \text{ mol m}^{-3})$, $L_{21}^r = f(\bar{C}_1, \bar{C}_2 = 37.71 \text{ mol m}^{-3})$, $L_{13}^r = f(\bar{C}_1, \bar{C}_2 = \text{const.})$ and $L_{31}^r = f(\bar{C}_1, \bar{C}_2 = \text{const.})$ ($r = A$ or *B*) for membrane system in concentration polarization condition (graphs 1A, 1B, 2A and 2B) and in homogeneous solutions (graphs 1 and 2).

Graphs 1 and 2 obtained for coefficients L_{12}, L_{21}, L_{21}^A and L_{21}^B show that the values of these coefficients increase linearly with an increase of $\bar{C}_1$. The values of these coefficients are the same ($L_{12} = L_{21} = L_{21}^A = L_{21}^B$) for homogeneous solutions and in concentration polarization conditions and do not depend on the configuration of the membrane system. The graphs 1A and 1B show that values of coefficients L_{12}^A and L_{12}^B increase nonlinearly with an increase of $\bar{C}_1$ and are dependent on the configuration of the membrane system. For $\bar{C}_1 < 49.7$ mol m^{-3} $L_{12}^A > L_{12}^B$, for $\bar{C}_1 = 49.7$ mol m^{-3} $L_{12}^A = L_{12}^B = 2.38 \times 10^{-10}$ mol N^{-1} s^{-1} and for $\bar{C}_1 > 49.7$ mol m^{-3} $L_{12}^A < L_{12}^B$.

Graphs 2A and 2B illustrating concentration dependencies of L_{13}^A and L_{13}^B were obtained for configurations *A* and

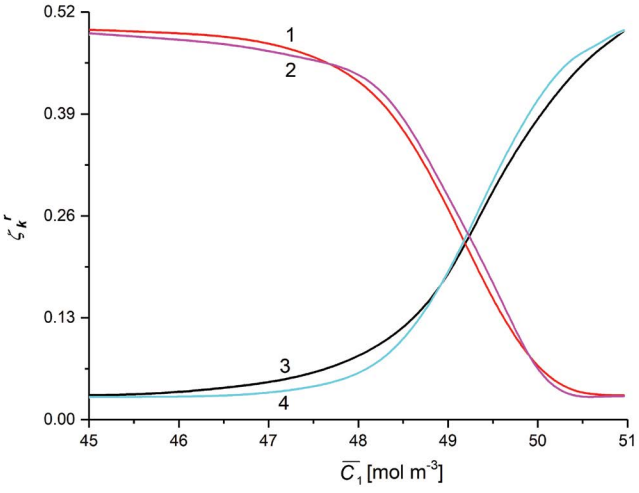

Fig. 5. Coefficients ζ_k^r as functions of mean glucose concentration in membrane ($\bar{C}_1$) and $\bar{C}_2 = 37.7$ mol m^{-3} for: ζ_1^B (1), ζ_v^B (2), ζ_1^A (3) and ζ_v^A (4).

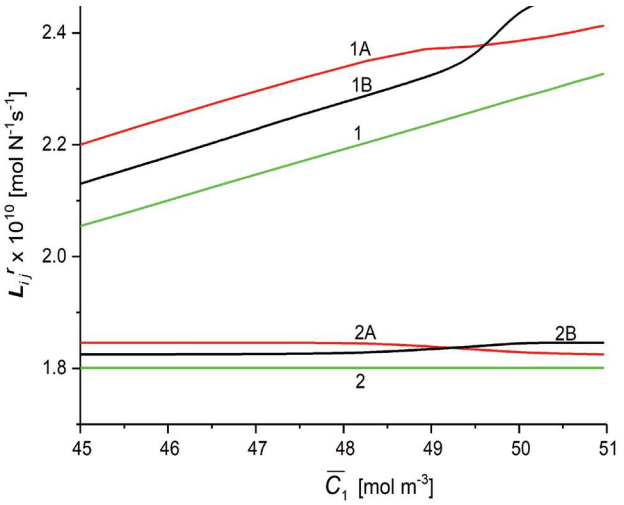

Fig. 6. Coefficients L_{ij}^r as functions of mean glucose concentration in membrane for $\bar{C}_2$ = 37.7 mol m^{-3}: L_{12}^A (1A), L_{12}^B (1B), L_{12}, L_{21} L_{21}^A, L_{21}^A (1), L_{13}^A (2A), L_{13}^B (2B) and L_{13} (2).

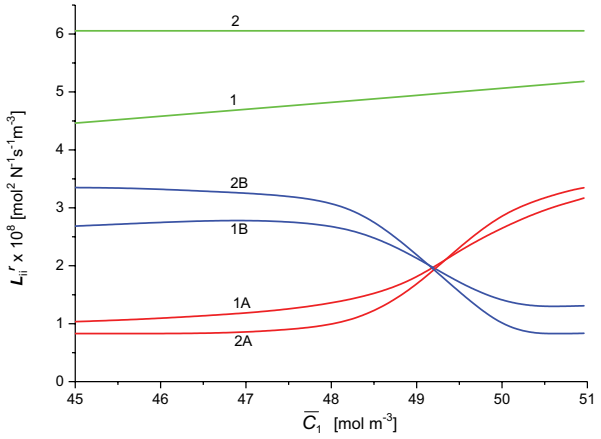

Fig. 7. Coefficients L_{ii}^r (i = 2 or 3) as functions of mean glucose concentration in membrane for $\bar{C}_2$ = 37.7 mol m^{-3}: L_{22}^A (1A), L_{22}^B (1B), L_{22} (1), L_{33}^A (2A), L_{33}^B (2B) and L_{33} (2).

B of the membrane system respectively. In the case of configuration A, for $\bar{C}_1 \le 47.3$ mol m^{-3} the value of the coefficient is constant and equal to $L_{13}^A = 1.85 \times 10^{-10}$ mol N^{-1} s^{-1}. For $\bar{C}_1 > 45.4$ mol m^{-3}, L_{13}^A decreases nonlinearly to $L_{13}^A = 1.82 \times 10^{-10}$ mol N^{-1} s^{-1}. In the case of configuration B, for $\bar{C}_1 \le 45.4$ mol m^{-3} the value of the coefficient is constant and equal to $L_{13}^B = 1.85 \times 10^{-10}$ mol N^{-1} s^{-1}. For $\bar{C}_1 > 45.4$ mol m^{-3}, L_{13}^B increases nonlinearly to $L_{13}^B = 1.85 \times 10^{-10}$ mol N^{-1} s^{-1}. Besides, from this figure it appears that, for $\bar{C}_1 < 49.3$ mol m^{-3}, $L_{13}^A > L_{13}^B > L_{13}$, for $\bar{C}_1 > 49.3$ mol m^{-3} $L_{13}^B > L_{13}^A > L_{13}$, and for $\bar{C}_1 = 49.3$ mol m^{-3} $L_{13}^A = L_{13}^B = 1.84 \times 10^{-10}$ mol N^{-1} s^{-1}.

The concentration dependencies of L_{22}^r and L_{33}^r ($r = A$ or B) presented in Fig. 7 for the membrane system in concentration polarization conditions for $\bar{C}_2$ = 37.7 mol m^{-3} were calculated on the basis of Eq. (4) taking into account the concentration dependencies shown in Fig. 5.

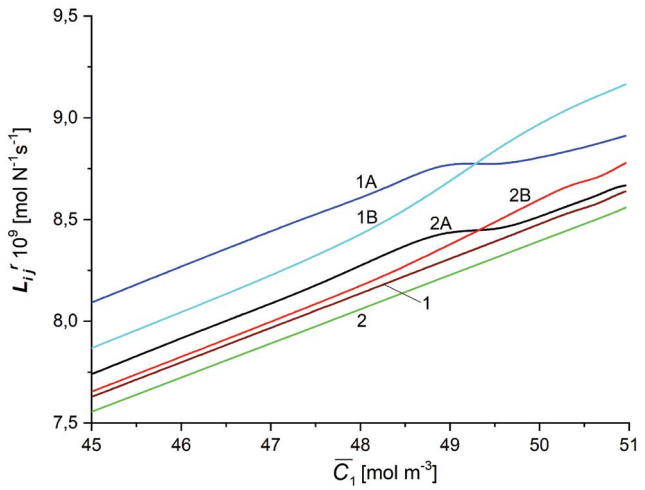

Fig. 8. Coefficients L_{ij}^r as functions of mean glucose concentration in membrane for $\bar{C}_2$ = 37.7 mol m^{-3}: L_{32} (1), L_{32}^A (1A), L_{32}^B (1B), L_{23} (2), L_{23}^A (2A) and L_{23}^B (2B).

In the case of configuration A the value of coefficient L_{22}^A increases nonlinearly from $L_{22}^A = 1.08 \times 10^{-8}$ mol^2 N^{-1} s^{-1} m^{-3} (for $\bar{C}_1 = 45.4$ mol m^{-3}, $\bar{C}_2 = 37.7$ mol m^{-3}) to $L_{22}^A = 3.17 \times 10^{-8}$ mol^2 N^{-1} s^{-1} m^{-3} (for $\bar{C}_1$ = 50.96 mol m^{-3}, $\bar{C}_2$ = 37.7 mol m^{-3}). The value of coefficient L_{22}^B in configuration B of the membrane system decreases nonlinearly from $L_{22}^B = 2.56 \times 10^{-8}$ mol^2 N^{-1} s^{-1} m^{-3} (for $\bar{C}_1$ = 46.5 mol m^{-3}, $\bar{C}_2$ = 37.7 mol m^{-3}) to $L_{22}^B = 1.31 \times 10^{-8}$ mol^2 N^{-1} s^{-1} m^{-3} (for $\bar{C}_1 = 50.96$ mol m^{-3}). Besides $L_{22}^A = L_{22}^B = 1.98 \times 10^{-8}$ mol^2 N^{-1} s^{-1} m^{-3} for $\bar{C}_1 = 49.3$ mol m^{-3} and $\bar{C}_2$ = 37.7 mol m^{-3}. For homogeneous solutions $L_{22}^A = L_{22}^B = L_{22}$ increase linearly from $L_{22} = 4.47 \times 10^{-8}$ mol^2 N^{-1} s^{-1} m^{-3} to $L_{22} = 5.18 \times 10^{-8}$ mol^2 N^{-1} s^{-1} m^{-3}. Besides, from this figure it can be seen that $L_{22}^A < L_{22}^B < L_{22}$ (for $\bar{C}_1 < 49.3$ mol m^{-3}), $L_{22}^B < L_{22}^A < L_{22}$ (for $\bar{C}_1 > 49.3$ mol m^{-3}) and $L_{22}^A = L_{22}^B$ (for $\bar{C}_1 = 49.3$ mol m^{-3}).

Graphs 2A and 2B illustrating dependencies L_{33}^A and L_{33}^B were obtained for configurations A and B of the membrane system, respectively. In the case of configuration A, for $\bar{C}_1 \le 46.6$ mol m^{-3} the value of coefficient is constant and equal to $L_{33}^A = 0.83 \times 10^{-9}$ mol^2 N^{-1} s^{-1} m^{-3}. For $\bar{C}_1 > 46.6$ mol m^{-3}, L_{33}^A increases nonlinearly to $L_{33}^A = 3.35 \times 10^{-9}$ mol^2 N^{-1} s^{-1} m^{-3}. In the case of configuration B, for $\bar{C}_1 \le 46.6$ mol m^{-3} the value of coefficient is constant and equal to $L_{33}^B = 3.35 \times 10^{-9}$ mol^2 N^{-1} s^{-1} m^{-3}. For $\bar{C}_1 > 46.6$ mol m^{-3}, L_{33}^B decreases nonlinearly to $L_{33}^B = 0.83 \times 10^{-9}$ mol^2 N^{-1} s^{-1} m^{-3}. For homogeneous solutions $L_{33}^A = L_{33}^B = L_{33} = 6.05 \times 10^{-9}$ mol^2 N^{-1} s^{-1} m^{-3} in whole range of studied $\bar{C}_1$. Besides, from this figure it appears that, for $\bar{C}_1 < 49.3$ mol m^{-3}, $L_{33}^A < L_{33}^B < L_{33}$, for $\bar{C}_1 > 49.3$ mol m^{-3} $L_{33}^B < L_{33}^A < L_{33}$, and for $\bar{C}_1 = 49.3$ mol m^{-3} $L_{33}^A = L_{33}^B = 1.95 \times$ mol^2 N^{-1} s^{-1} m^{-3}.

The graphs shown in Fig. 8 illustrate the concentration dependencies of L_{ij}^r ($i \ne j \in \{2, 3\}$, $r = A$ or B) for the membrane system in concentration polarization conditions.

The graphs in Fig. 8 show that the values of the coefficients L_{23}^A and L_{23}^B increase nonlinearly with the increase of $\bar{C}_1$ and are dependent on the configuration of the membrane system. For $\bar{C}_1 < 49.3$ mol m^{-3} $L_{23}^A > L_{23}^B$, for $\bar{C}_1 = 49.3$ mol m^{-3} $L_{23}^A = L_{23}^B = 8.5 \times 10^{-9}$ mol N^{-1} s^{-1}, and $L_{23}^B > L_{23}^A$ for $\bar{C}_1 > 49.3$ mol m^{-3}. Similar relations are observed for the

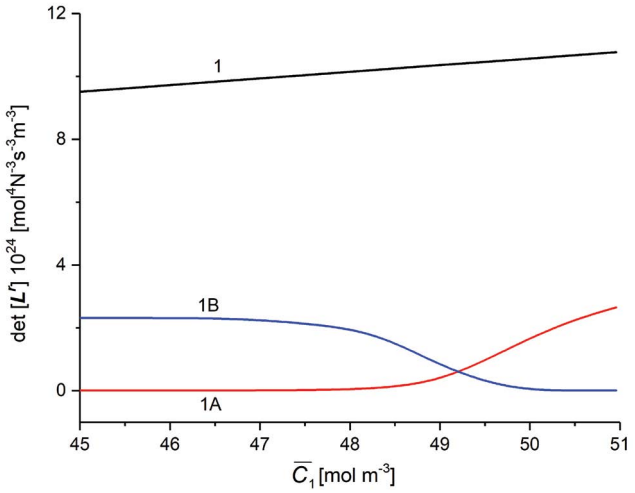

Fig. 9. Det[L^r] as functions of mean glucose concentration in membrane for $\bar{C}_2$ = 37.7 mol m^{-3}: det[L^A] (1A), det[L^B] (1B) and det[L] (1).

coefficients L^A_{32} and L^B_{32}. The lines for the coefficients L_{23} and L_{32} obtained for homogeneous solutions indicate that the values of these coefficients increase linearly with an increase of $\bar{C}_1$ and do not depend on the configuration of the membrane system. Besides, from this figure it can be seen that for $\bar{C}_1$ < 49.3 mol m^{-3} a relationship takes place $L^A_{32} > L^B_{32} > L^A_{23} > L^B_{23} > L_{32} > L_{23}$ and for $\bar{C}_1$ > 49.3 mol m^{-3} – $L^B_{32} > L^A_{32} > L^B_{23} > L^A_{23} > L_{32} > L_{23}$.

The concentration dependencies of det[L^r] (i, j ∈ {1, 2, 3}, r = A or B) shown in Fig. 9 for homogeneous solutions (graph 1) and concentration polarization conditions (graphs 1A and 1B) were calculated on the basis of Eq. (5) after taking into account the concentration dependencies of ζ^r_1 and ζ^r_2 presented in Fig. 5.

Graphs 1A and 1B which illustrate the dependencies det[L^A] and det[L^B] were obtained suitably for configurations A and B of the membrane system. In the case of configuration A the value of det[L^A] for $\bar{C}_1$ < 48.3 mol m^{-3} is constant and equal to det[L^A] = 0.004 × 10^{-24} mol^4 N^{-3} s^{-3} m^{-3}. For $\bar{C}_1$ > 48.3 mol m^{-3} det[L^A] increases nonlinearly and for $\bar{C}_1$ = 50.96 mol m^{-3} reaches the value det[L^A] = 2.65 × 10^{-24} mol^4 N^{-3} s^{-3} m^{-3}. In the case of configuration B the value det[L^B] decreases from det[L^B] = 2.34 × 10^{-24} mol^4 N^{-3} s^{-3} m^{-3} (for $\bar{C}_1$ = 45.5 mol m^{-3}) to det[L^B] = 0.009 × 10^{-24} mol^4 N^{-3} s^{-3} m^{-3} (for $\bar{C}_1$ = 50.96 mol m^{-3}). Besides det[L^A] = det[L^B] = 0.53 × 10^{-24} mol^4 N^{-3} s^{-3} m^{-3} for $\bar{C}_1$ = 49.3 mol m^{-3}, for $\bar{C}_1$ < 49.3 mol m^{-3}, det[L^A] < det[L^B] and for $\bar{C}_1$ > 49.3 mol m^{-3}, det[L^A] > det[L^B]. For homogeneous solutions det[L] increases linearly from det[L] = 10.5 × 10^{-24} mol^4 N^{-3} s^{-3} m^{-3} (for $\bar{C}_1$ = 45.5 mol m^{-3}) to det[L] = 10.8 × 10^{-24} mol^4 N^{-3} s^{-3} m^{-3} (for $\bar{C}_1$ = 50.9 mol m^{-3}). Moreover, from this figure it appears that, for $\bar{C}_1$ < 49.3 mol m^{-3}, det[L^A] < det[L^B] < det[L], for $\bar{C}_1$ > 49.3 mol m^{-3} det[L^B] < det[L^A] < L_{33}.

The results of the study presented in Figs. 6–9 show that the values of L^r_{12}, L^r_{13}, L^r_{22}, L^r_{23}, L^r_{32}, L^r_{33} and det[L^r] calculated for the conditions of concentration polarization are determined by hydrodynamic conditions (diffusion or diffusion–convective conditions) in solutions near the membrane, which separates ternary non-electrolytes solution with different concentrations of solutes. This means that the values of these coefficients in concentration polarization conditions depend strongly on both concentrations $\bar{C}_1$ and $\bar{C}_2$ as well as the configuration of the membrane system. However, in the case of mechanical stirring of solutions, the values of these coefficients do not depend on the membrane system configuration. Therefore, for interpretation of results of calculation, the combinations of coefficients L^A_{ij}, L^B_{ij} and L_{ij} (i, j ∈ {1, 2, 3}) of the same indicators and det[L^A], det[L^B] and det[L] were used. These combinations are presented by Eqs. (8)–(13). Concentration dependencies of new coefficients facilitate the location of areas differentiated by hydrodynamic conditions in near membrane areas such as diffusion, convection–diffusion and convection. For transport coefficient of the membrane as a function of glucose concentration we also observe the criss-crosses of characteristics for configuration A and B in points with glucose concentration similar to analogous dependencies of concentration polarization coefficients (49.3 mol m^{-3}).

3.3. Calculations of the coefficients ϕ_{ij} and ϕ_{det}

To calculate coefficients ϕ_{ij} and ϕ_{det} based on Eqs. (8) and (9) we used the characteristics $L^r_{ij} = f(\bar{C}_1, \bar{C}_2 = 37.7 \text{ mol m}^{-3})$, ($i$, j ∈ {1, 2, 3}, r = A, B) presented in Figs. 6–9. The graphs presented in Fig. 10 were calculated on the basis of Eqs. (8) and (9).

In the case of curves 1′ and 2′ the values of coefficients ϕ_{12} and ϕ_{32} for $\bar{C}_1$ < 45.7 mol m^{-3} are constant and amounts $\phi_{12} \approx \phi_{32}$ = 0.03. For $\bar{C}_1$ > 45.7 mol m^{-3} values of coefficients ϕ_{12} and ϕ_{32} decreases nonlinearly to $\phi_{12} \approx \phi_{32}$ = –0.03 (for $\bar{C}_1$ = 50.96 mol m^{-3}). Besides, from this figure it follows that $\phi_{32} = \phi_{12}$ = 0, for $\bar{C}_1$ = 49.3 mol m^{-3}, respectively. For $\bar{C}_1$ < 49.3 mol m^{-3} $\phi_{12} \approx \phi_{32} > 0$. In turn for $\bar{C}_1$ > 49.3 mol m^{-3} $\phi_{12} \approx \phi_{32} > 0$.

In the case of curves 3′ and 4′ the values of coefficients ϕ_{13} and ϕ_{23} for $\bar{C}_1$ < 45.7 mol m^{-3} are constant and amount $\phi_{13} = \phi_{23}$ = 0.012. For $\bar{C}_1$ > 45.7 mol m^{-3} values of coefficients ϕ_{12} and ϕ_{32} decrease nonlinearly to ϕ_{12} = –0.012 and ϕ_{23} = –0.013 (for, $\bar{C}_1$ = 50.9 mol m^{-3}). Besides, from this figure it follows that $\phi_{23} = \phi_{13}$ = 0, for $\bar{C}_1$ = 49.3 mol m^{-3}, respectively. For $\bar{C}_1$ < 49.3 mol m^{-3} $\phi_{32} > 0$, $\phi_{12} > 0$ and $\phi_{23} < \phi_{13}$. In turn for $\bar{C}_1$ > 49.3 mol m^{-3} $\phi_{23} < 0$, $\phi_{13} < 0$ and $\phi_{23} > \phi_{13}$.

Graphs 1–3 presented in Fig. 10 illustrates the concentration dependencies of ϕ_{22}, ϕ_{33} = and ϕ_{det} calculated on the basis of Eqs. (8) and (9), respectively. Curve 1 shows that value of coefficient ϕ_{22} initially increases linearly from ϕ_{22} = –0.41 (for $\bar{C}_1$ = 45.5 mol m^{-3}) to ϕ_{22} = –0.37 (for $\bar{C}_1$ = 45.6 mol m^{-3}), and next increases nonlinearly to value ϕ_{22} = 0.36 (for $\bar{C}_1$ = 50.9 mol m^{-3}). In the case of curve 2 the values of coefficient ϕ_{33} for $\bar{C}_1$ < 45.6 mol m^{-3} are constant and amount ϕ_{33} = –0.42. Moreover, for $\bar{C}_1$ = 49.3 mol m^{-3}, $\phi_{22} = \phi_{33}$ = 0, for $\bar{C}_1$ < 49.3 mol m^{-3}, $\phi_{22} < 0$ and $\phi_{33} < 0$, and for $\bar{C}_1$ > 49.3 mol m^{-3}, $\phi_{22} > 0$ and $\phi_{33} > 0$. In turn, curve 3 shows that values of coefficient ϕ_{det} for $\bar{C}_1$ < 45.6 mol m^{-3} are constant and amount ϕ_{det} = –0.25. Moreover, for $\bar{C}_1$ = 49.3 mol m^{-3}, ϕ_{det} = 0, for $\bar{C}_1$ < 49.3 mol m^{-3}, $\phi_{det} < 0$, and for $\bar{C}_1$ > 49.3 mol m^{-3}, $\phi_{det} > 0$.

The criss-cross of concentration characteristics of diagonal ϕ coefficients as functions of glucose concentration is

observed for a similar concentration of glucose as previously analyzed coefficients. The values of ϕ coefficients at criss-cross equals zero. It means that the change of sign of ϕ coefficients during changing of glucose concentration is caused by a change of conditions of CBLs rebuilding.

From presented considerations, it results that the coefficients ϕ_{12}, ϕ_{32}, ϕ_{13}, ϕ_{23}, ϕ_{22} and ϕ_{det} are a measure of the convective effect. Assuming that $\zeta_p^r = \zeta_{a1}^r = \zeta_{a2}^r = 1$, $\zeta_{s11}^r = \zeta_{s12}^r = \zeta_1^r$ and $\zeta_{s22}^r = \zeta_{s21}^r = \zeta_2^r$, from Eq. (8) it follows that the ϕ_{11}, ϕ_{21} and ϕ_{31} coefficients can only be zero. In turn from Eqs. (8) and (9) it follows that the values of coefficients ϕ_{12}, ϕ_{32}, ϕ_{13}, ϕ_{23}, ϕ_{22}, ϕ_{33} and ϕ_{det} can be smaller, equal to or greater than zero.

In order to show that the values of coefficients ϕ_{12}, ϕ_{32}, ϕ_{13}, ϕ_{23}, ϕ_{22}, ϕ_{33} and ϕ_{det} are equal to or greater than zero, it is enough to replace the sign "<" with "=" or ">". The "<" or ">" signs imply the return of the convective flux directed in accordance with or oppositely to the vector of gravitation $\bar{g}$. If the condition $\phi_{12} = \phi_{32} = \phi_{13} = \phi_{23} = \phi_{22} = \phi_{33} = \phi_{det} = 0$ is satisfied, this means that the system is at the critical point: the CBLs system loses stability, but natural convection does not occur yet. This means that the membrane system is not sensitive to changes of gravitational field. This is illustrated by the dependencies $\phi_{12} = f(\bar{C}_1, \bar{C}_2 = 37.7 \text{ mol m}^{-3})$, $\phi_{32} = f(\bar{C}_1, \bar{C}_2 = 37.7 \text{ mol m}^{-3})$, $\phi_{13} = f(\bar{C}_1, \bar{C}_2 = 37.7 \text{ mol m}^{-3})$, $\phi_{23} = f(\bar{C}_1, \bar{C}_2 = 37.7 \text{ mol m}^{-3})$, $\phi_{22} = f(\bar{C}_1, \bar{C}_2 = 37.7 \text{ mol m}^{-3})$, $\phi_{33} = f(\bar{C}_1, \bar{C}_2 = 37.7 \text{ mol m}^{-3})$, and $\phi_{det} = f(\bar{C}_1, \bar{C}_2 = 37.7 \text{ mol m}^{-3})$, presented in Fig. 10 and interferograms presented in the previous paper [27]. Besides, the hydrodynamic stability in the membrane system is connected with the concentration Rayleigh number (R_C) [25,28–30]. The value of R_C depends on the concentration of solutes separated by the membrane [26]. For points, in which $\phi_{12} = 0$, $\phi_{32} = 0$, $\phi_{13} = 0$, $\phi_{23} = 0$, $\phi_{22} = 0$ or $\phi_{det} = 0$, the critical value of R_C can be determined on the basis of expression $R_C = [g(\rho_h - \rho_l)D_{11}^2(1 - \zeta)^3][8\rho_h\nu_h(\zeta 8RT\omega_{11})^3]^{-1}$ [26,27]. Taking into consideration $D_{11} = 0.69 \times 10^{-9}$ m^2 s^{-1}, $g = 9.81$ m s^{-2}, $\omega_{11} = 0.8 \times 10^{-9}$ mol N^{-1} s^{-1}, $\nu = 1.06 \times 10^{-6}$ m^2 s^{-1}, $\rho_h = 998.7$ kg m^{-3}, $\rho_l = 998.3$ kg m^{-3} and $\zeta = 0.23$ in this expression, we get $(R_C)_{crit.} \approx 1{,}130$. This value corresponds to the

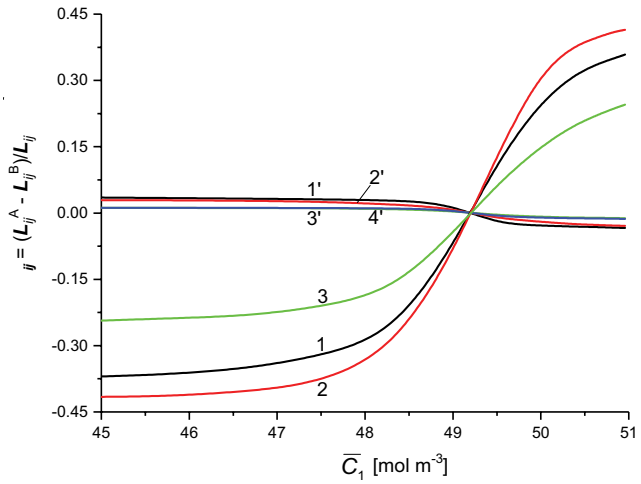

Fig. 10. Coefficients ϕ_{ij} as functions of mean glucose concentration in the membrane for $\bar{C}_2 = 37.7$ mol m^{-3}: ϕ_{12} (1′), ϕ_{32} (2′), ϕ_{23} (3′), ϕ_{13} (4′), ϕ_{22} (1), ϕ_{33} (2) and ϕ_{det} (3).

$(R_C)_{crit.} = 1100.6$, obtained for the case of the rigid membrane surface and the free liquid interior (rigid-free borders) [31].

Using the conditions $\zeta_p^r = \zeta_{a1}^r = \zeta_{a2}^r = 1$, $\zeta_{s11}^r = \zeta_{s12}^r = \zeta_1^r$ and $\zeta_{s22}^r = \zeta_{s21}^r = \zeta_2^r$, the Eqs. (4) and (8) can be written in the form containing the thickness of the boundary layer (δ^A and δ^B). For example, the equation for ϕ_{22} can be written as – Eq. (14):

$$\phi_{22} = \frac{\left[\omega_{11} - L_p\bar{C}_1\sigma_1\left(1-\sigma_1\right)\left(\zeta_1^A - \zeta_1^B\right)\right]}{\left[\omega_{11} + L_p\bar{C}_1\left(1-\sigma_1\right)^2\right]} \tag{14}$$

From this equation it follows that if $\zeta_1^A = \zeta_1^B$, then $\phi_{22} = 0$. Moreover, taking into account the Eq. (14) and the expressions $\zeta_1^A = D_1(D_1 + 2RT\omega_{11}\delta^A)^{-1}$ and $\zeta_1^B = D_1(D_1 + 2RT\omega_{11}\delta^B)^{-1}$ it can be shown that:

$$\zeta_1^A - \zeta_1^B = \frac{2D_1RT\omega_{11}\left(\delta^B - \delta^A\right)}{\left(D_1 + 2RT\omega_{11}\delta^A\right)\left(D_1 + 2RT\omega_{11}\delta^A\right)} \tag{15}$$

In the aforementioned equation, δ^A and δ^B can be determined by laser interferometry [30] or volume flux measurements [26].

Fig. 10 shows that for the coefficients ϕ_{12}, ϕ_{23}, ϕ_{32} and ϕ_{13} the condition $-0.035 \le \phi_{ij} \le +0.035$ is fulfilled. In turn, for the coefficients ϕ_{22}, ϕ_{33} and ϕ_{det} the condition $-0.41 \le \phi_{ij} \le +0.41$ is fulfilled. The curves in Fig. 10 have sigmoidal shapes, for coefficients with symmetrical indexes ϕ_{ii} and ϕ_{det} are increasing functions of $\bar{C}_1$ while coefficients with non-symmetrical indexes ϕ_{ij}, $i \neq j$ are decreasing functions of $\bar{C}_2$. The values of all ϕ_{ij} coefficients are in the range from –0.5 to 0.5. The characteristic point of all curves is for glucose concentration of 49.2 m^3 mol m^{-3}. At this point, the values of all coefficients are equal zero and all curves intersect at this point. Besides this point is the inflection point of all curves. Table 1 contains derivative $\frac{\partial\phi_{ij}}{\partial\bar{C}_1}$ at this point, calculated for all graphs presented in Fig. 10.

As results from Fig. 10 and Table 1, the absolute values of changes of coefficients with different indexes in this same range of glucose concentration are much lower than for coefficients with these same indexes. Besides absolute values of derivatives of coefficients with different indexes over the glucose concentration at point $\bar{C}_{1o} = 49.2$ mol m^{-3} is also much lower than derivatives of coefficients with this same indexes.

3.4. Calculations of the coupling coefficients l_{ij} and l_{ij}^r

The coupling coefficients l_{ij} and l_{ij}^r were calculated based on Eqs. (10) and (11) and the respective concentration dependencies of L_{ij}^r and L_{ij} ($i, j \in \{1, 2, 3\}$, $r = A, B$) presented in Figs. 6–8. The l_{ij}^r and l_{ij} coefficients as functions of glucose concentration ($\bar{C}_1$) for the constant value of ethanol concentration ($\bar{C}_2 = 37.7$ mol m^{-3}) at the initial moment are shown in Fig. 11.

Graphs 1 and 2 in Fig. 11 show the dependencies of l_{23} and l_{32} on glucose concentration in membrane. From these graphs it results that the values l_{23} and l_{32} for 45 mol m^{-3} ≤ $\bar{C}_1$ ≤ 51 mol m^{-3} are constant and equal $l_{23} = 0.14$ and $l_{32} = 0.15$ suitably. In turn graphs 1A, 1B, 2A and 2B

show nonlinear dependencies, respectively for: l^A_{23}, l^B_{23}, l^A_{32} and l^B_{32}. For 45 mol m^{-3} ≤ $\bar{C}_1$ ≤ 51 mol m^{-3} the values l^A_{23}, l^B_{23} and l^A_{23}, l^B_{23} fulfil relationships 0.83 ≤ l^A_{23} ≤ 0.26, 0.25 ≤ l^B_{23} ≤ 0.83, 0.86 ≤ l^A_{32} ≤ 0.27 and 0.26 ≤ l^B_{32} ≤ 0.86. The graphs 1A and 2A intersect at the coordinate point $\bar{C}_1$ = 49.2 mol m^{-3} and l^A_{23} = l^B_{23} = 0.43, while the curves 1B and 2B – at the coordinate point $\bar{C}_1$ = 49.2 mol m^{-3} l^A_{32} = l^B_{32} = 0.45. The graphs 5 and 3 in Fig. 11 show the dependencies l_{13} and l_{31} on glucose concentration in membrane, respectively. The values of l_{13} and l_{31} for 45 mol m^{-3} ≤ $\bar{C}_1$ ≤ 51 mol m^{-3} are constant and equal l_{13} = l_{31} = 0.33. The graphs 5A and 5B show the nonlinear dependencies, respectively for l^A_{13} and l^B_{13}. For 45 mol m^{-3} ≤ $\bar{C}_1$ ≤ 51 mol m^{-3} the values l^A_{13} and l^B_{13} fulfil relationships 0.45 ≤ l^A_{13} ≤ 0.9 and 0.9 ≤ l^B_{13} ≤ 0.46. The graphs 3A and 3B show the nonlinear dependencies, respectively for l^A_{31} and l^B_{31}. For 45 mol m^{-3} ≤ $\bar{C}_1$ ≤ 51 mol m^{-3} the values l^A_{31} and l^B_{31} fulfil relationships 0.44 ≤ l^A_{31} ≤ 0.88 and 0.88 ≤ l^A_{31} ≤ 0.44. These graphs intersect at the coordinate point $\bar{C}_1$ = 49.3 mol m^{-3} and l^A_{13} = l^B_{13} = 0.59 and l^A_{31} = l^B_{31} = 0.6. Graph 4 in Fig. 11 shows linear dependence of l_{12} and graph 6 linear dependence of l_{21} = l^A_{21} = l^B_{21}. The values of l_{12} for 45 mol m^{-3} ≤ $\bar{C}_1$ ≤ 51 mol m^{-3} fulfil relationship 0.44 ≤ l_{12} ≈ l_{21} = l^A_{21} = l^B_{21} ≤ 0.46. Graphs 4B and 4A show the nonlinear dependence, respectively for l^A_{12} and l^B_{12}. For 45 mol m^{-3} ≤ $\bar{C}_1$ ≤ 51 mol m^{-3} the values l^A_{12} and l^B_{12} fulfil relationships 0.98 ≤ l^A_{12} ≤ 0.61 and 0.59 ≤ l^B_{12} ≤ 0.98. These graphs intersect at the coordinate point $\bar{C}_1$ = 49.2 mol m^{-3} and l^A_{12} = l^B_{12} = 0.76. From Fig. 11 it results that 0.14 ≤ l_{21} ≤ 0.46, 0.25 ≤ l^B_{ij} ≤ 0.97 and 0.97 ≤ l^A_{ij} ≤ 0.26. In addition, for $\bar{C}_1$ = 45 mol m^{-3} the following relationships are satisfied: l_{23} = l_{32} < l^B_{23} < l^B_{32} < l_{13} < l_{31} < l_{12} = l_{21} = l^A_{21} = l^B_{21} < l^B_{31} < l^B_{13} < l^B_{12} < l^A_{23} < l^A_{32} < l^A_{31} < l^A_{13} < l^A_{12} and for $\bar{C}_1$ = 51 mol m^{-3}: l_{23} = l_{32} < l^A_{23} < l^A_{32} < l_{13} < l_{31} < l^A_{31} < l^A_{13} < l_{12} < l_{21} = l^A_{21} = l^B_{21} < l^A_{12} < l^B_{23} < l^B_{32} < l^B_{31} < l^B_{13} < l^B_{12}.

The graphs in Fig. 11 have characteristic shapes, dependent on the configuration of the membrane system and homogeneity of solutions. In the case of homogeneous solutions (mechanically stirred solutions – black lines 1, 2, 5, 3, 4 and 6) the coefficients do not depend on the configuration of the membrane system and are linearly dependent on the glucose concentration. Stirring of solutions with a suitable high rate of stirring causes that during transport of solution through the membrane the CBLs do not appear and the fluxes through the membrane and forces on the membrane are maximal. In the case of non-homogeneous solutions (without stirring of solutions in chambers) appearance of CBLs near membrane causes that the suitable fluxes and forces on the membrane are lower than in the case of homogeneous solutions. This causes that the coefficients for suitable solute concentrations are higher than in homogeneous conditions. Besides the coupling coefficients for non-homogeneous conditions strongly depend on the membrane configuration. In *A* configuration, an increase of glucose concentration with constant ethanol concentration at the initial moment causes a decrease of coupling coefficients. The range of greater changes of these coefficients is for glucose concentration from 48 to 51 mol m^{-3}. In *B* configuration, an increase of glucose concentration causes an increase of coupling coefficients. The range of glucose concentrations for which the change of coupling coefficients in *B* configuration is maximal is in the range similar to *A* configuration of the membrane system. Values of all coupling coefficients fulfill the conditions 0 ≤ l_{ij} ≤ +1 and 0 ≤ l^r_{ij} ≤ +1, specified by Kedem and Caplan [16]. Analyzing the characteristics of coupling coefficients in non-homogeneous conditions we observed that for appropriate characteristics in *A* and *B* configurations of the membrane system the crisscross of suitable pairs of characteristics (1A and 1B, 2A and 2B, 5A and 5B, 3A and 3B, 4B and 4A) is observed at the concentration 49.2 mol m^{-3}. For this concentration of glucose, the densities of ternary solutions in upper and lower chambers at the initial moment are the same. In this case, we also observed the appearance of hydrodynamic instabilities which causes disturbance of diffusive reconstruction of CBLs near the membrane. Despite the fact that the densities of solutions at the initial moment were this same the diffusion of glucose and ethanol through the membrane caused the appearance of concentration gradients (and density gradients) in CBLs suitably high and directed oppositely to gravitation acceleration that the hydrodynamic instabilities can appear in the membrane system.

Table 1
Derivative $\frac{\partial \phi_{ij}}{\partial \bar{C}_1}$ at point $\bar{C}_{1o}$ = 49.2 mol m^{-3}, for graphs presented in Fig. 10

Graph	$\frac{\partial \phi_{ij}}{\partial \bar{C}_1}$ (mol m^{-3})
1	0.357
2	0.423
3	0.203
1′	–0.078
2′	–0.04
3′	–0.0263
4′	–0.0163

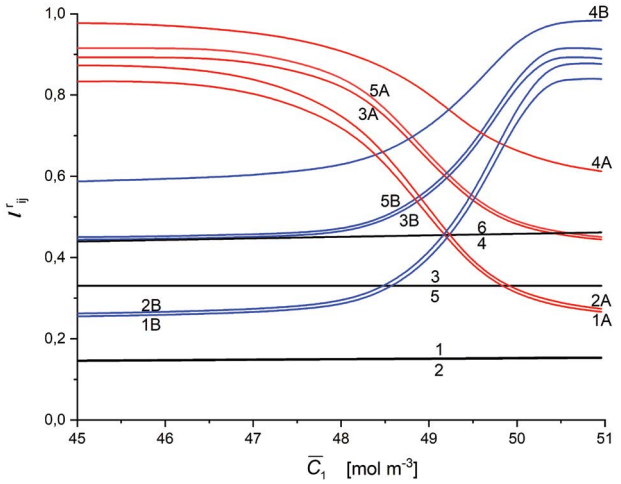

Fig. 11. The l^r_{ij} and l_{ij} coefficients as functions of glucose concentration for l_{23} (1), l^A_{23} (1A), l^B_{23} (1B), l_{32} (2), l^A_{32} (2A), l^B_{32} (2B), l_{31} (3), l^A_{31} (3A), l^B_{31} (3B), l_{12} (4), l^A_{12} (4A), l^B_{12} (4B), l_{13} (5), $l_{13}{}^A$ (5A), l^B_{13} (5B) and l_{21} = l^A_{21} = l^B_{21} (6).

3.5. Evaluation of energy conversion efficiency

To calculate coefficients $e_{ij} = f(\bar{C}_1, \bar{C}_2 = 37.7 \text{ mol m}^{-3})$ and $e_{ij}^r = f(\bar{C}_1, \bar{C}_2 = 37.7 \text{ mol m}^{-3})$ based on Eqs. (12)–(13) we used the respective concentration dependencies of $l_{ij} = f(\bar{C}_1, \bar{C}_2 = 37.7 \text{ mol m}^{-3})$ and $l_{ij}^r = f(\bar{C}_1, \bar{C}_2 = 37.7 \text{ mol m}^{-3})$ ($i, j \in \{1, 2, 3\}$, $r = A, B$) presented in Figs. 6–8. The results of calculations are shown in Fig. 12.

Graphs 1 and 2 in Fig. 12 show that $e_{23} = e_{32} = 0.005$. In turn graphs 1A, 1B, 2A and 2B show nonlinear dependencies, respectively for: l_{23}^A, l_{23}^B, l_{32}^A and l_{32}^B. For 45 mol m^{-3} ≤ $\bar{C}_1$ ≤ 51 mol m^{-3} the values l_{23}^A, l_{23}^B and l_{23}^A, l_{23}^B fulfil relationships $0.3 \le e_{23}^A \le 0.017$, $0.015 \le e_{23}^B \le 0.31$, $0.31 \le e_{32}^A \le 0.02$ and $0.016 \le e_{32}^B \le 0.32$. Graphs 1A and 1B intersect at the coordinate point $\bar{C}_1$ = 49.2 mol m^{-3} and $e_{23}^A = e_{23}^B = 0.059$, while the curves 2A and 2B – at the coordinate point $\bar{C}_1$ = 49.2 mol m^{-3} $e_{32}^A = e_{32}^B = 0.065$. The graphs 3 and 4 in Fig. 11 show that $e_{13} = e_{31} = 0.029$. Graphs 3A and 3B show the nonlinear dependencies, respectively for e_{13}^A and e_{13}^B. For 45 mol m^{-3} ≤ $\bar{C}_1$ ≤ 51 mol m^{-3} the values e_{13}^A and e_{13}^B fulfil relationships $0.414 \le e_{13}^A \le 0.056$ and $0.056 \le l_{13}^A \le 0.406$. Graphs 4A and 4B show the nonlinear dependencies, respectively for e_{31}^A and e_{31}^B. For 45 mol m^{-3} ≤ $\bar{C}_1$ ≤ 51 mol m^{-3} the values e_{31}^A and e_{31}^B fulfil relationships $0.392 \le e_{31}^A \le 0.055$ and $0.055 \le e_{31}^B \le 0.338$. These graphs intersect at the coordinate point $\bar{C}_1$ = 49.3 mol m^{-3} and $e_{13}^A = e_{13}^B = 0.11$ and $e_{31}^A = e_{31}^B = 0.12$. Graphs 5 and 6 in Fig. 11 show linear dependences $e_{12} \approx e_{21} = e_{21}^A = e_{21}^B$. The values of these coefficients for 45 mol m^{-3} ≤ $\bar{C}_1$ ≤ 51 mol m^{-3} fulfil relationship $0.054 \le e_{12} \approx e_{21} = e_{21}^A = e_{21}^B \le 0.061$. Graphs 5B and 5A show the nonlinear dependence, respectively for e_{12}^A and e_{12}^B. For 45 mol m^{-3} ≤ $\bar{C}_1$ ≤ 51 mol m^{-3} the values e_{12}^A and e_{12}^B fulfil relationships $0.3 \le e_{12}^A \le 0.11$ and $0.1 \le e_{12}^B \le 0.32$. These graphs intersect at the coordinate point $\bar{C}_1$ = 49.2 mol m^{-3} and $e_{12}^A \cdot e_{12}^B = 0.18$. From Fig. 11 it results that $0.005 \le e_{ij} \le 0.061$, $0.015 \le e_{ij}^B \le 0.41$ and $0.414 \le e_{ij}^A \le 0.017$. Besides for $\bar{C}_1$ = 45 mol m^{-3} the following relations are fulfilled: $e_{23} = e_{32} < e_{23}^B < e_{32}^B < e_{13} < e_{31} < e_{12} = e_{21} < e_{21}^B < e_{31}^B < e_{13}^B < e_{21}^A < e_{12}^B < e_{23}^A < e_{12}^A < e_{32}^A < e_{31}^A < e_{13}^A$ and for $\bar{C}_1$ = 51 mol m^{-3}, $e_{23} = e_{32} < e_{23}^A < e_{32}^A < e_{13} < e_{31} < e_{31}^A < e_{13}^A < e_{12} = e_{21} = e_{21}^A = e_{21}^B < e_{12}^A < e_{23}^B < e_{12}^B < e_{32}^B < e_{31}^B < e_{13}^B$.

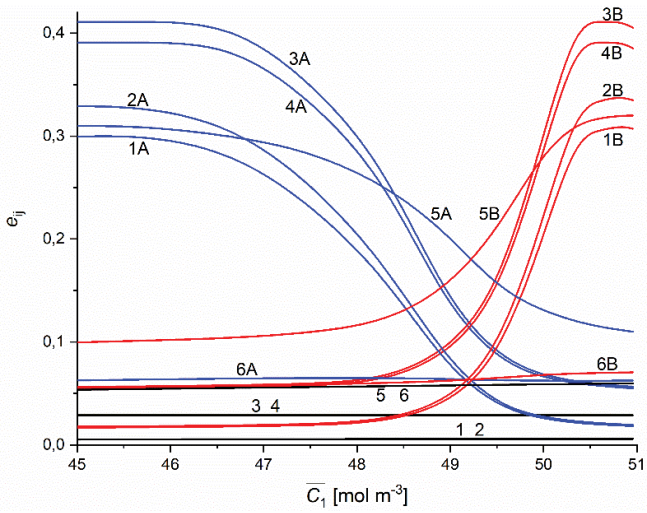

Fig. 12. The e_{ij}^r coefficients as functions of glucose concentration for: e_{23} (1), e_{23}^A (1A), e_{23}^B (1B), e_{32} (2), e_{32}^A (2A), e_{32}^B (2B), e_{13} (3), e_{13}^A (3A), e_{13}^B (3B), e_{31} (4), e_{31}^A (4A), e_{31}^B (4B), e_{12} (5), e_{12}^A (5A), e_{12}^B (5B), e_{21} (6), e_{21}^A (6A) and e_{21}^B (6B).

Nowadays, membrane separation is increasingly used in water and wastewater technology, and the research into membrane transport is the subject of scientific considerations of a number of scientists all over the world [32–36]. Therefore, in scientific research centers, the multidirectional research is being conducted, not only into the separation of single- or multi-component solutions but also the development of highly selective membrane materials.

4. Conclusions

Research has shown that:

- In order to describe transport processes of ternary solutions of non-electrolytes through horizontally oriented membrane nine Peusner's coefficients should be calculated L_{ij}^r ($i, j \in \{1, 2, 3\}$, $r = A, B$) and determinant of the matrix of these coefficients det[L^r].
- For Nephrophan membrane and aqueous solutions of glucose the values of coefficients L_{12}^r, L_{13}^r, L_{21}^r, L_{22}^r, L_{23}^r, L_{31}^r, L_{32}^r and L_{33}^r are dependent on concentration and configuration of the membrane system and these coefficients fulfill the relations $L_{12}^r \ne L_{21}^r$, $L_{13}^r \ne L_{31}^r$ and $L_{23}^r \ne L_{32}^r$.
- Concentration dependencies of coefficients $\phi_{ij} = (L_{ij}^A - L_{ij}^B)/L_{ij}$ and $\phi_{\text{det}} = (\det[L^A] - \det[L^B])/\det[L])$ facilitate estimation of natural convection direction: for $\phi_{ij} < 0$ or $\phi_{\text{det}} < 0$ natural convection is directed vertically upwards and for $\phi_{ij} > 0$ or $\phi_{\text{det}} > 0$ – vertically downwards.
- Value of coefficients ϕ_{ij} and ϕ_{det} ($\phi_{ij} < 0$, $\phi_{\text{det}} < 0$, $\phi_{ij} = 0$, $\phi_{\text{det}} = 0$, $\phi_{ij} > 0$ or $\phi_{\text{det}} > 0$) shows the influence of concentration polarization and natural convection on the membrane transport.
- The coupling (l_{ij}^r) and energy conversion (e_{ij}^r) coefficients linearly depend on glucose concentrations for mechanically stirred solutions while in concentration polarization condition they nonlinearly depend on the glucose concentration in the membrane. Increase of glucose concentration in the membrane causes an increase of these coefficients in the case of configuration *A* while decreases of these coefficients in case of configuration *B*. The crisscross of suitable *A* and *B* characteristics are observed at glucose concentration $\bar{C}_1$ = 49.2 mol m^{-3}.
- The Kedem–Katchalsky model, as a research tool, can be used for the research into membrane transport in environmental engineering and, in particular, for the description of the separation of solution components in water purification processes (e.g. desalination of water, marine water separation) and wastewater treatment.

Acknowledgment

The scientific research was funded by the statute subvention of Czestochowa University of Technology.

Symbols

l_{ij} — Degree of coupling for diluted and homogeneous solutions

J_k^r — Solute flux in non-homogeneous conditions, mol m^{-2} s^{-1}
J_i — Thermodynamic fluxes in homogeneous conditions
l_{ij}^r — Degree of coupling for diluted and non-homogeneous solutions
e_{ij} — Energy conversion efficiency for diluted and homogeneous solutions
e_{ij}^r — Energy conversion efficiency for diluted and non-homogeneous solutions
J_v^r — Volume flux in non-homogeneous conditions, m s^{-1}
L_{ij}^r — Symmetric Peusner's coefficients for non-homogeneous solutions
J_i^r — Thermodynamic fluxes in non-homogeneous conditions
X_i^r — Thermodynamic forces in non-homogeneous conditions
X_i — Thermodynamic forces in homogeneous conditions
$\bar{C}_k$ — Mean solute concentration in the membrane, mol m^{-3}
l_h^r, l_l^r — Concentration boundary layers, CBLs
C_{ki}^r, C_{ke}^r — Concentrations of solutions at interfaces: l_h^r/M and M/l_l^r
$l_h^r/M/l_l^r$ — Complex CBL/*M*/CBL
C_{kh}, C_{kl} — Concentrations of solutions in chambers of the membrane system
D_A, D_B — Diffusion coefficient in configurations *A* and *B*, m^2 s^{-1}
J_k — Solute flux in homogeneous conditions, mol m^{-2} s^{-1}
J_v — Volume flux in homogeneous conditions, m s^{-1}
L_{ij} — Symmetric Peusner's coefficients for homogeneous ternary solutions
L_p — Hydraulic permeability coefficient, m^3 N^{-1} s^{-1}
P_h, P_l — Hydrostatic pressures (*h* higher and *l* lower value), Pa
R_C — Concentration Rayleigh number
RT — Product of the gas constant and thermodynamic temperature, J mol^{-1}
ΔP — Hydrostatic pressure difference, Pa

Greek letters

$\Delta\pi$ — Osmotic pressure difference, Pa
σ — Reflection coefficient
δ_h^r, δ_l^r — Thickness of concentration boundary layers in configurations *A* and *B* of membrane system, m
ω_{ks} — Solute permeability coefficient, mol N^{-1} s^{-1}
ζ_p — Hydraulic concentration polarization coefficient
ζ_v — Osmotic concentration polarization coefficient
ζ_s — Diffusive concentration polarization coefficient
ζ_a — Advective concentration polarization coefficient
ζ_{ks}^r — Concentration polarization coefficient
ρ_l, ρ_h — Densities of solutions outside of CBLs, kg m^{-3}
ρ_i^r, ρ_e^r — Densities of solutions at the interfaces: l_h^r/M and M/l_l^r, kg m^{-3}

References

[1] Y. Demirel, V. Gerbaud, Nonequilibrium Thermodynamics: Transport and Rate Processes in Physical, Chemical and Biological Systems, Elsevier, Amsterdam, 2014.
[2] M. Aguilella-Arzo, M. Queralt-Martín, M.-L. Lopez, A. Alcaraz, Fluctuation-driven transport in biological nanopores. A 3D Poisson–Nernst–Planck study, Entropy, 19 (2017) e19030116.
[3] Z. Siwy, F. Fornasiero, Improving on aquaporins, Science, 357 (2017) 753
[4] B.Y. Huang, H.K. Wang, B.X. Yang, Water Transport Mediated by Other Membrane Proteins, B.X. Young, Ed., Aquaporins. Advances in Experimental Medicine and Biology, Vol. 969, Springer, Dordrecht, 2017, pp. 251–261.
[5] V.V. Nikonenko, A.V. Kovalenko, M.K. Urtenov, N.D. Pismenskaya, J.Y. Han, P. Sistat, G. Pourcelly, Desalination at overlimiting currents: state-of-the-art and perspectives, Desalination, 342 (2014) 85–106.
[6] S.J. Park, H.J. Kim, D.H. Seol, T.J. Park, M. Leem, H.W. Ha, H.S. An, H. You Kim, S.-J. Jeong, S.J. Park, H.S. Kim, Y.S. Kim, Evenly transferred single-layered graphene membrane assisted by strong substrate adhesion, Nanotechnology, 28 (2017) 145706.
[7] A. Katchalsky, P.F. Curran, Nonequilibrium Thermodynamics in Biophysics, Harvard, Cambridge, 1965.
[8] H.Y. Elmoazzen, J.A.W. Elliot, L.E. McGann, Osmotic transport across cell membranes in nondilute solutions: a new nondilute solute transport equation, Biophys. J., 96 (2009) 2559–2571.
[9] O. Kedem, A. Katchalsky, Thermodynamic analysis of the permeability of biological membranes to non-electrolytes, Biochim. Biophys. Acta, 27 (1958) 229–246.
[10] I.W. Richardson, E.A.D. Foster, S. Miękisz, Nonlinear generalizations of the Kedem–Katchalsky equations for ionic fluxes, Bull. Math. Biol., 44 (1982) 761–775.
[11] X. Cheng, P.M. Pinsky, The balance of fluid and osmotic pressures across active biological membranes with application to the corneal endothelium, PLoS One, 10 (2015) e0145422.
[12] S.S.S. Cardoso, J.H.E. Cartwright, Dynamics of osmosis in a porous medium, R. Soc. Open Sci., 1 (2017) 140352.
[13] A. Kargol, A mechanistic model of transport processes in porous membranes generated by osmotic and hydrostatic pressure, J. Membr. Sci., 191 (2001) 61–69.
[14] M. Kargol, A. Kargol, Mechanistic formalism for membrane transport generated by osmotic and mechanical pressure, Gen. Physiol. Biophys., 22 (2003) 51–68.
[15] L. Peusner, Studies in Network Thermodynamics, Elsevier, Amsterdam, 1986.
[16] O. Kedem, S.R. Caplan, Degree of coupling and its relation to efficiency of energy conversion, Trans. Faraday Soc., 61 (1965) 1897–1911.
[17] K.M. Batko, I. Ślęzak-Prochazka, S. Grzegorczyn, A. Ślęzak, Membrane transport in concentration polarization conditions: network thermodynamics model equations, J. Porous Media, 17 (2014) 573–586.
[18] K.M. Batko, I. Ślęzak-Prochazka, A. Ślęzak, Network form of the Kedem–Katchalsky equations for ternary non-electrolyte solutions. 2. Evaluation of L_{ij} Peusner's coefficients for polymeric membrane, Polim. Med., 43 (2013) 103–109.
[19] A. Ślęzak, S. Grzegorczyn, K.M. Batko, Resistance coefficients of polymer membrane with concentration polarization, Transp. Porous Media, 95 (2012) 151–170.
[20] K.M. Batko, I. Ślęzak-Prochazka, A. Ślęzak, Network hybrid form of the Kedem–Katchalsky equations for non-homogenous binary non-electrolyte solutions: evaluation of P_{ij}^* Peusner's tensor coefficients, Transp. Porous Media, 106 (2015) 1–20.
[21] I. Ślęzak-Prochazka, K.M. Batko, S. Wąsik, A. Ślęzak, H^* Peusner's form of the Kedem–Katchalsky equations for on-homogeneous non-electrolyte binary solutions, Transp. Porous Media, 111 (2016) 457–477.
[22] K.M. Batko, A. Ślęzak, Membrane transport of non-electrolyte solutions in concentration polarization conditions: H^r form of

the Kedem–Katchalsky–Peusner equations, Int. J. Chem. Eng., 2019 (2019) 10 pages, https://doi.org/10.1155/2019/5629259.
[23] A. Ślęzak, Irreversible thermodynamic model equations of the transport across a horizontally mounted membrane, Biophys. Chem., 34 (1989) 91–102.
[24] A. Ślęzak, S. Grzegorczyn, J. Jasik-Ślęzak, K. Michalska-Małecka, Natural convection as an asymmetrical factor of the transport through porous membrane, Transp. Porous Media, 84 (2010) 685–698.
[25] K. Dworecki, A. Ślęzak, B. Ornal-Wąsik, S. Wąsik, Effect of hydrodynamic instabilities on solute transport in a membrane system, J. Membr. Sci., 265 (2005) 94–100.
[26] J.S. Jasik-Ślęzak, K.M. Olszówka, A. Ślęzak, Estimation of thickness of concentration boundary layers by osmotic volume flux determination, Gen. Physiol. Biophys., 30 (2011) 186–195.
[27] A. Ślęzak, K. Dworecki, I.H. Ślęzak, S. Wąsik, Permeability coefficient model equations of the complex: membrane-concentration boundary layers for ternary non-electrolyte solutions, J. Membr. Sci., 267 (2005) 50–57.
[28] A. Ślęzak, K. Dworecki, J. Jasik-Ślęzak, J. Wąsik, Method to determine the critical concentration Rayleigh number in isothermal passive membrane transport processes, Desalination, 168 (2004) 397–412.
[29] A. Ślęzak, K. Dworecki, J.E. Anderson, Gravitational effects on transmembrane flux: the Rayleigh—Taylor convective instability, J. Membr. Sci., 23 (1985) 71–81.
[30] K. Dworecki, S. Wąsik, A. Ślęzak, Temporal and spatial structure of the concentration boundary layers in a membrane system, Physica A, 326 (2003) 360–369.
[31] G. Lebon, D. Jou, J. Casas-Vasquez, Understanding Non-Equilibrium Thermodynamics. Foundations, Applications, Frontiers, Springer, Berlin, 2008.
[32] M. Bodzek, Chapter 15 – Membrane Technologies for the Removal of Micropollutants in Water Treatment, A. Basile, A. Cassano, N.K. Rastogi, Eds., Advances in Membrane Technologies for Water Treatment: Materials, Processes and Applications, Elsevier Science, Woodhead Publishing Ltd., Cambridge, 2015, pp. 465–517.
[33] M. Bodzek, M. Dudziak, K. Luks-Betlej, Application of membrane techniques to water purification. Removal of phthalates, Desalination, 162 (2004) 121–128.
[34] K. Mielczarek, J. Bohdziewicz, M. Włodarczyk-Makuła, M. Smol, Modeling performance of commercial membranes in the low-pressure filtration coking wastewater treatment based on mathematical filtration models, Desal. Water Treat., 52 (2014) 3743–3752.
[35] M. Dudziak, M. Bodzek, A study of selected phytoestrogens retention by reverse osmosis and nanofiltration membranes - the role of fouling and scaling, Chem. Pap., 64 (2010) 139–146.
[36] M. Wilf, L. Awerbuch, G. Pearce, C. Bartels, M. Mickley, N. Voutchkov, Membrane Desalination Technology, Balaban Desalination Publications, L'Aquila, Italy, 2006.